Supporting Information

Self-Healing Material with Reversible Luminescence Switch Behavior

Jing Yang, Tingting Wang, Ran Guo, Decui Yao, Weiwei Guo, Shuo Liu, Zhiqiang Li*, Yige Wang*, and Huanrong Li*

[a]National-Local Joint Engineering Laboratory for Energy Conservation in Chemical Process Integration and Resources Utilization, Tianjin Key Laboratory of Chemical Process Safety, School of Chemical Engineering and Technology, Hebei University of Technology, Guangrong Dao 8, Hongqiao District, Tianjin 300130, P. R. China.

[b]College of Chemistry, Nankai University, Tianjin 300350, P.R. China.

Table of Contents

1. Supporting Figures

2. Supporting Tables

Table S1. The $^5D_4$ lifetimes of Eu_xTb_y-Ppdc monitored at 543 nm and energy-transfer efficiency from Tb^{3+} to Eu^{3+} ions.

Table S2. The assignments of FT-IR spectra.

Table S3. The fracture energy evaluated from the curves in the Figure S20.

1. Supporting Figures

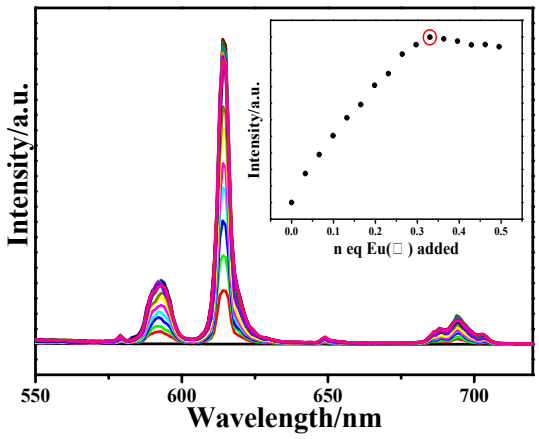

Figure S1. Emission spectra of Ppdc (1.0×10^{-5} M) upon addition of 0-0.5 equiv of $EuCl_3$ in ethanol at 25 °C (λ_{ex}=300 nm). Inset shows the emission intensity of $^5D_0 \rightarrow {}^7F_2$ change at 615 nm versus Eu^{3+}/ Ppdc molar ratio.

The coordination stoichiometry between Ppdc and Ln^{3+} was investigated by luminescence titration. As shown in Figure S1, upon stepwise addition of Eu^{3+}, the characteristic emission bands of Eu^{3+} contributed to $^5D_0 \rightarrow {}^7F_J$ (J = 0−4) transitions appeared and increased gradually. As shown in Figure S1 inset, the curve of emission intensity of $^5D_0 \rightarrow {}^7F_J$ at 615 nm shows an inflection point at a molar ratio of 0.33, corresponding to a 3:1 Ppdc/Eu^{3+} coordination complex.[1-2] Tb^{3+}-Ppdc was prepared and characterized according to the same method.

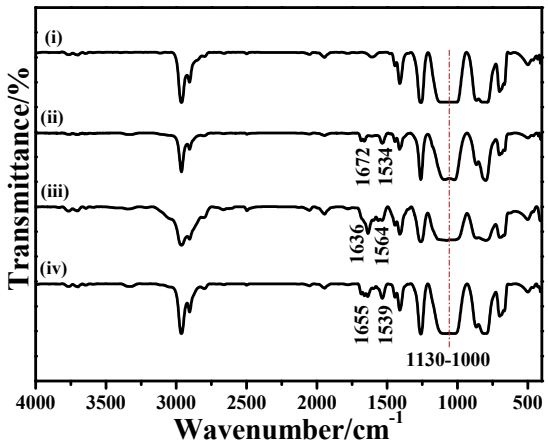

Figure S2. FT-IR spectra of (i) pdms, (ii) Ppdc, (iii) Eu-Ppdc, (iv) Tb-Ppdc.

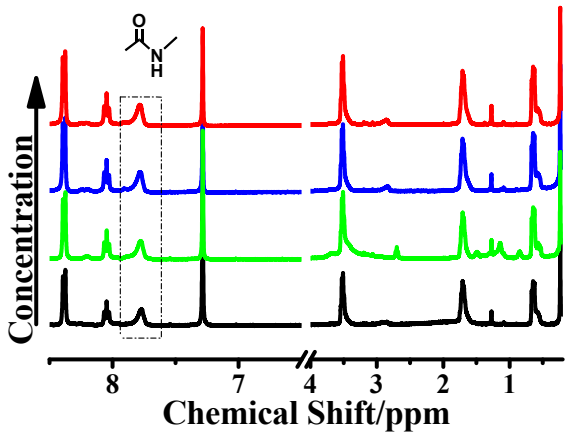

Figure S3. ^{1}H NMR spectra of Ppdc at various concentrations in $CDCl_3$.

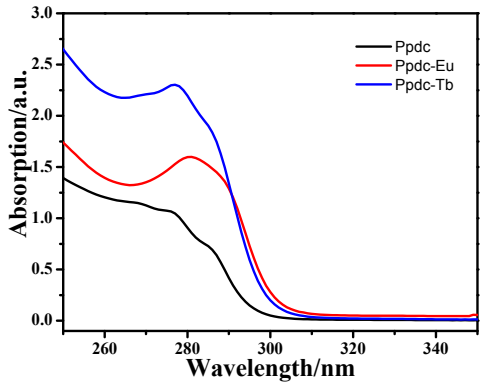

Figure S4. UV-Vis spectra of Ppdc, Eu-Ppdc and Tb-Ppdc in $CHCl_2$ with the concentration of 10^{-3}, 1.6×10^{-3} and 2.4×10^{-3} M, respectively.

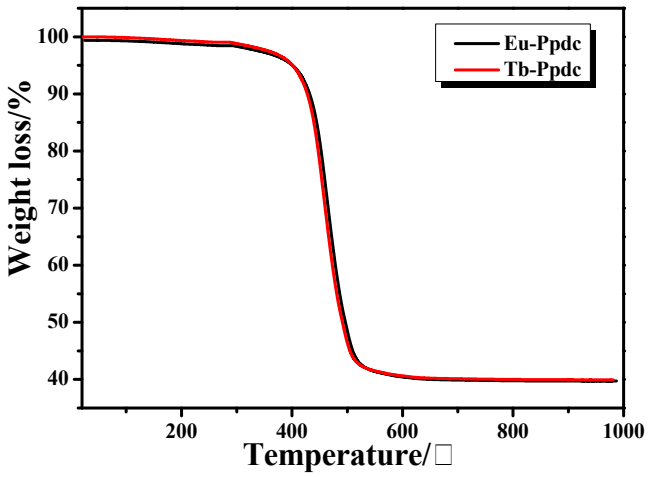

Figure S5. TGA curves of Ln-Ppdc.

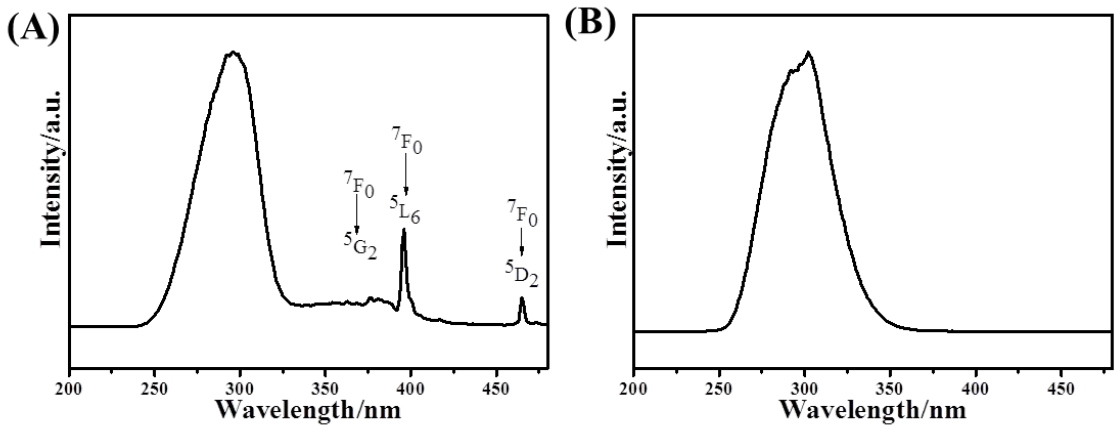

Figure S6. The excitation luminescence spectra of Eu-Ppdc (A) monitored at 615 nm and Tb-Ppdc (B) monitored at 543 nm.

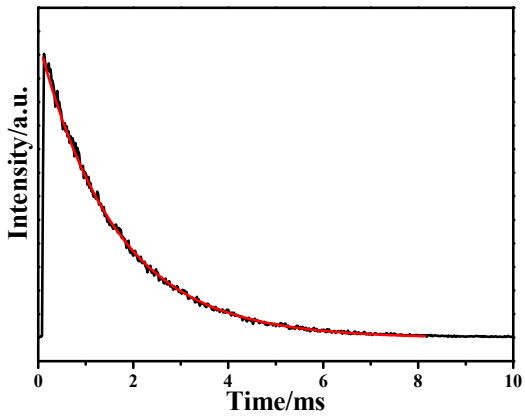

Figure S7. Decay curve of $^5D_4$ state (Tb^{3+} in Tb-Ppdc, λ_{ex} = 300 nm, $\lambda_{monitored}$ = 543 nm). The curve was fitted according to the single-exponential function ($I = I_0 + A \times \exp[-(t - t_0)/\tau]$).[3-4]

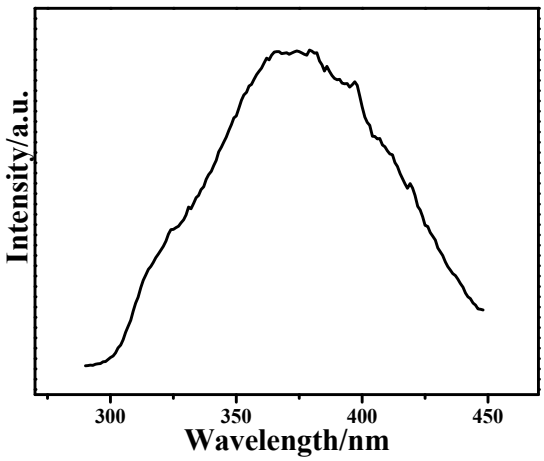

Figure S8. The excitation spectrum of Ppdc.

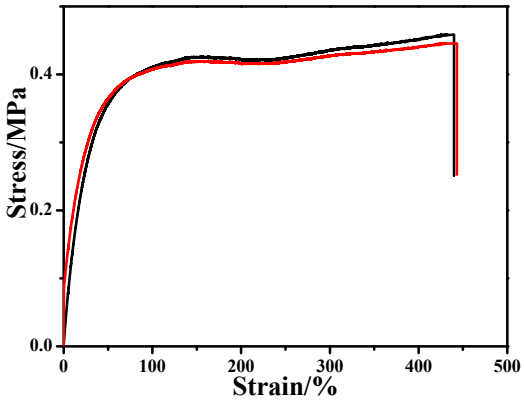

Figure S9. Stress–strain curves of Eu-Ppdc (black line) and Tb-Ppdc (red line).

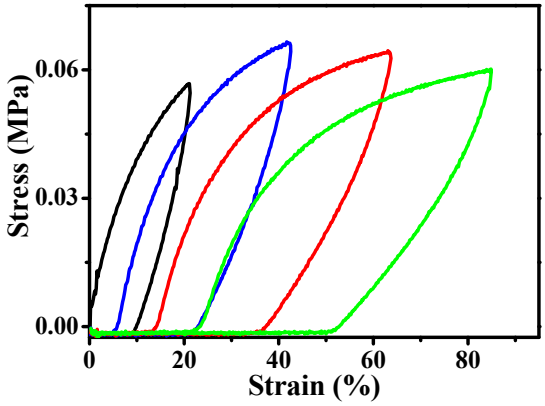

Figure S10. Eu-Ppdc was subjected to a cycle of loading and unloading to various strains. Black, blue, red and green lines represent the first to the fourth cycles, respectively (tensile rate: 100 mm min^{-1}).

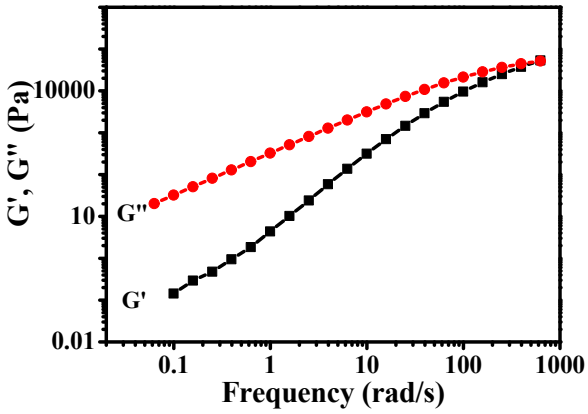

Figure S11. Frequency (ω) sweep tests at ω = 0.01–1000 rad s^{-1} and strain (γ) = 5% of Ppdc at room temperature.

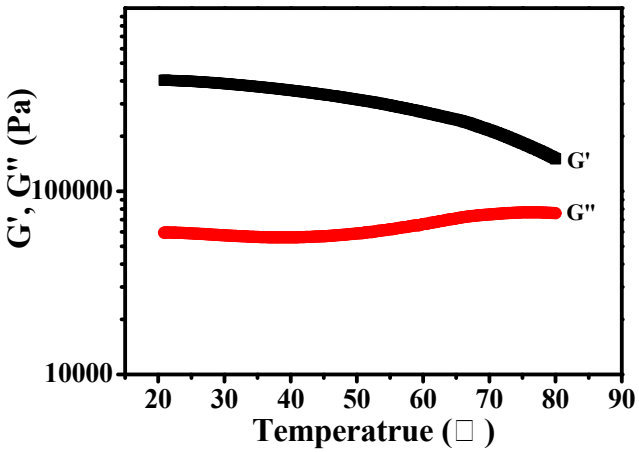

Figure S12. Storage modulus G' and loss modulus G'' of Eu-Ppdc versus temperature at ω = 1 Hz.

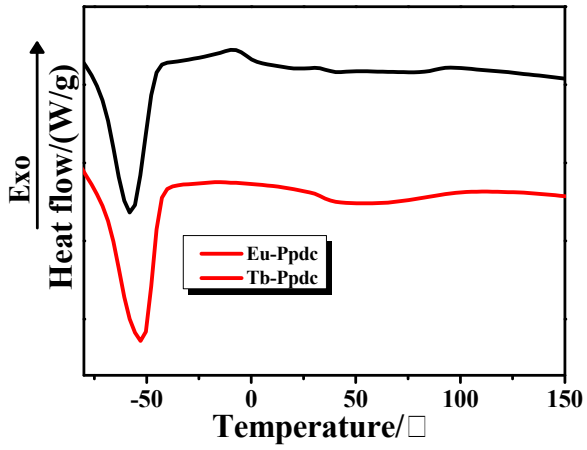

Figure S13. DSC curves of Ln-Ppdc.

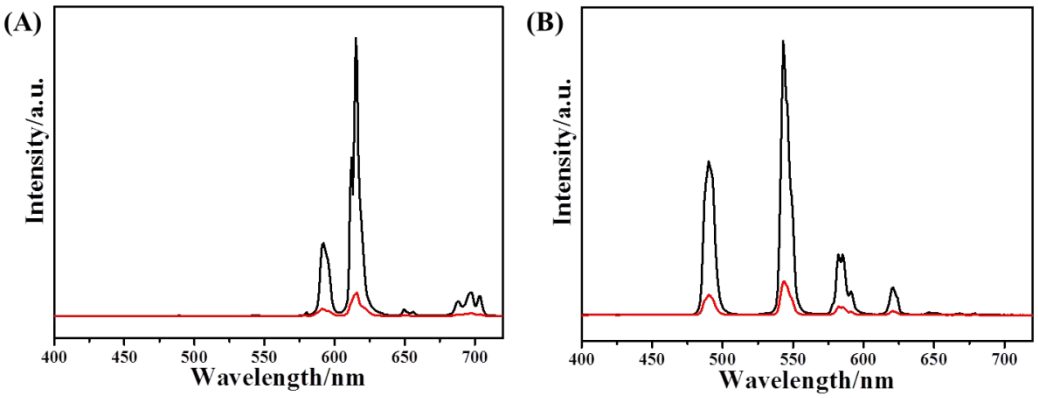

Figure S14. Emission spectra of (A) Eu-Ppdc and (B) Tb-Ppdc. They were obtained upon excitation at 300 nm, respectively. Red line and black line represent the materials upon TEA vapor and HCl gas, respectively.

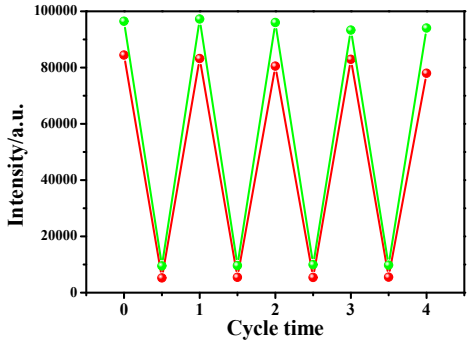

Figure S15. Responses of luminescence intensity at 615 nm of Eu-Ppdc (red line) and 543 nm of Tb-Ppdc (green line) during triethylamine−HCl exposure cycles.

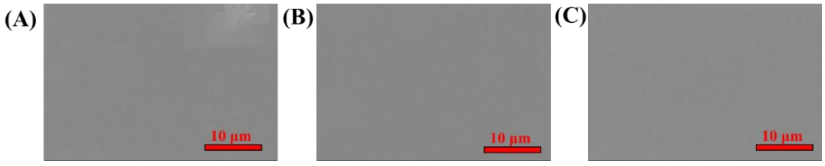

Figure S16. SEM images. (A): Eu-Ppdc, (B): Eu-Ppdc after TEA treatment, (C): (B) after HCl treatment.

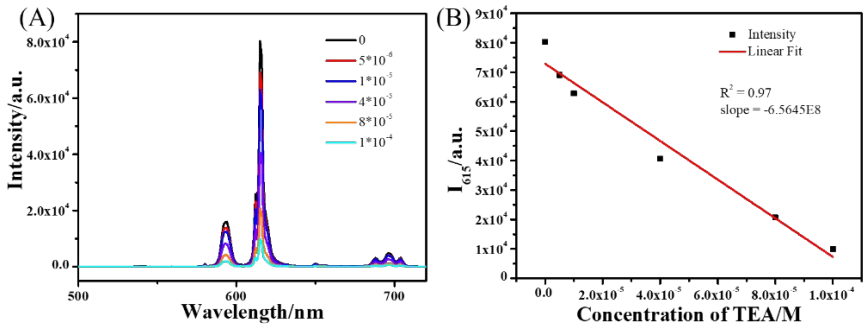

Figure S17. (A) Luminescence emission spectra of Ppdc-Eu after exposure different concentration of TEA and (B) their linear fit for the estimation of limit of detection.

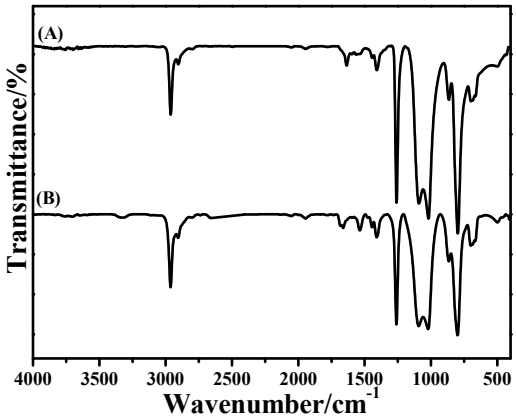

Figure S18. FT-IR spectra of Eu-Ppdc before (A) and after (B) exposure to TEA vapor.

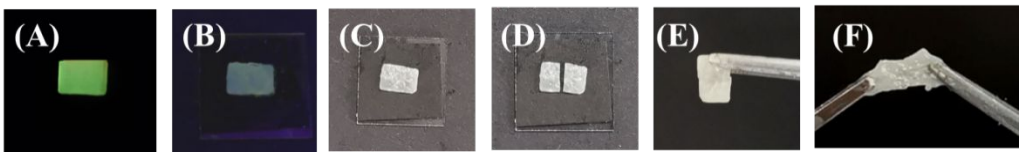

Figure S19. (A) and (B) represent Tb-Ppdc before and after exposure to TEA vapor under 302 nm UV irradiation, respectively. (C) is (B) under daylight. (D): cutting (C) into two peices. (E): the two peices healed to one. (F): stretching the healed one by hands. (C), (D), (E), and (F) are under daylight.

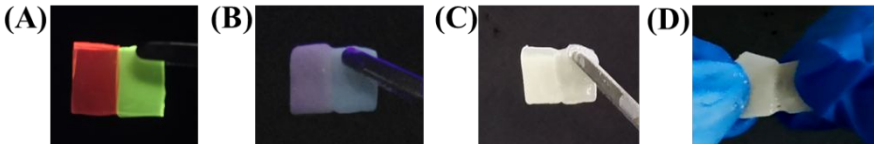

Figure S20. The healed one in the Figure 3 I iv before (A) and (B) after exposure to TEA vapor, they are under 302 nm UV irradiation. (C) is the (B) under daylight. (D): stretching (C) by hands, (C) and (D) are under daylight.

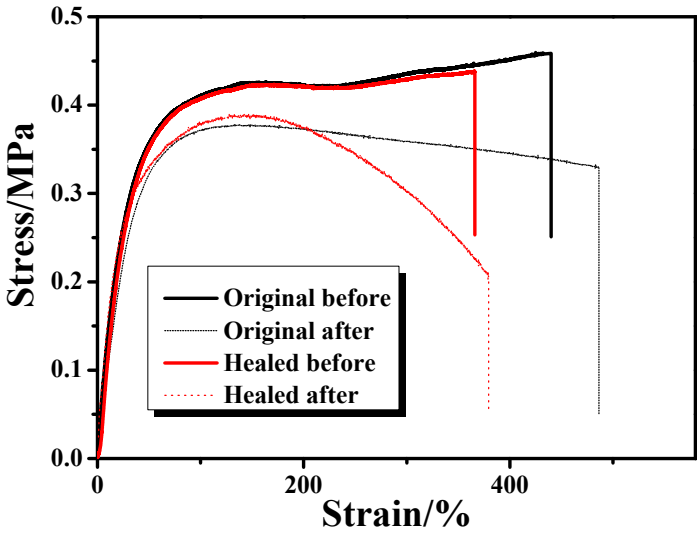

Figure S21. Stress-strain curves of the original (black solid line) and healed (red solid line) material after self-healing for 36 h before exposure to TEA, and their corresponding curves black short dots and red short dots after exposure to TEA. All the fracture energy evaluated from the curves as listed in Table S3.

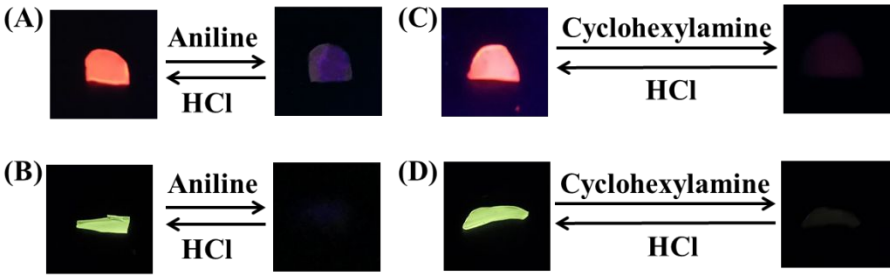

Figure S22. Ln-Ppdc as the switch adjusted by basic substances, such as aniline, cyclohexylamine. (A) and (C): Eu-Ppdc, (B) and (D): Tb-Ppdc.

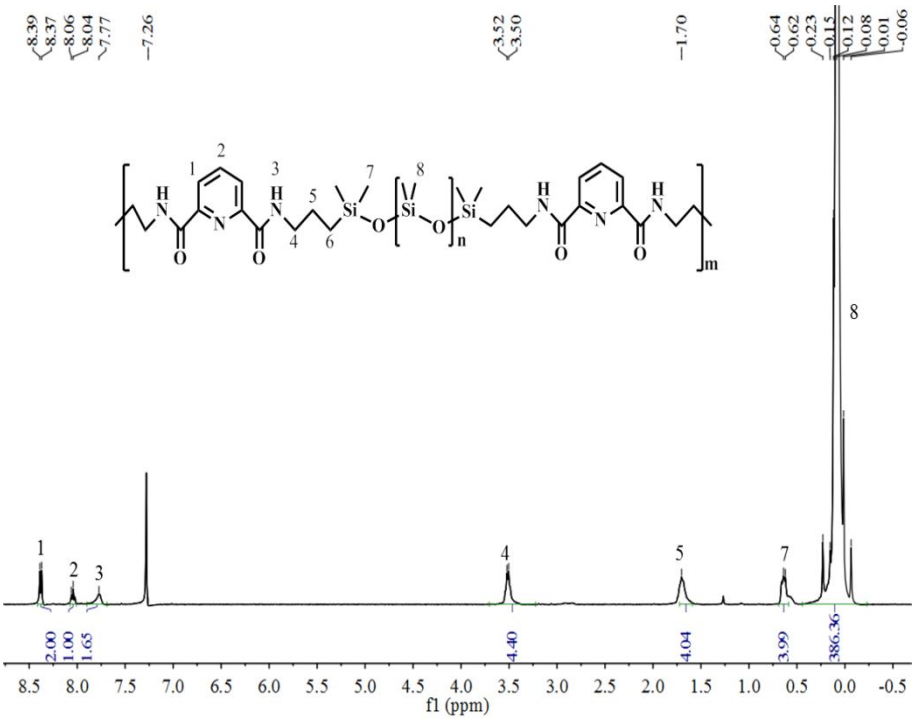

Figure S23. ^{1}H NMR spectrum of Ppdc.

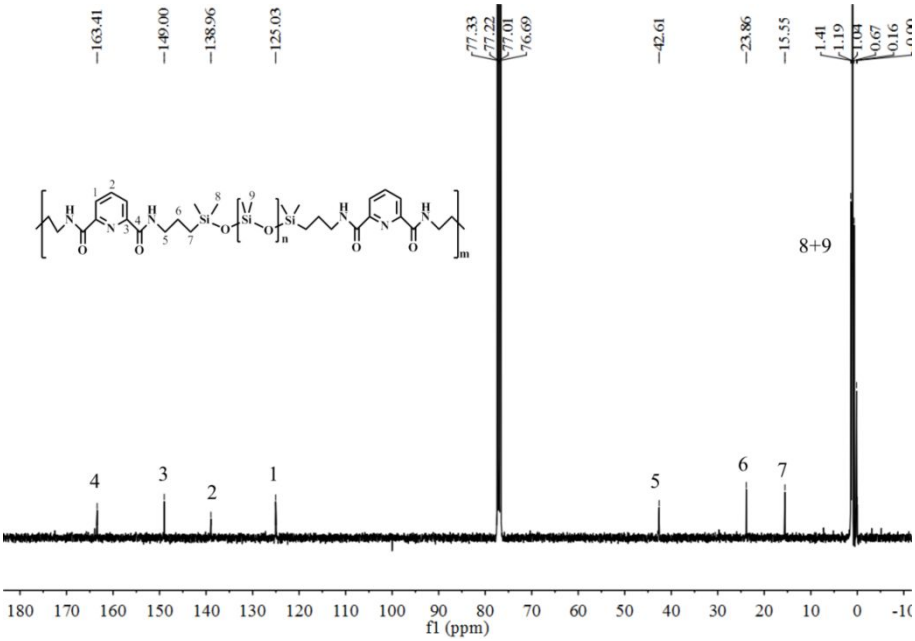

Figure S24. ^{13}C NMR spectrum of Ppdc.

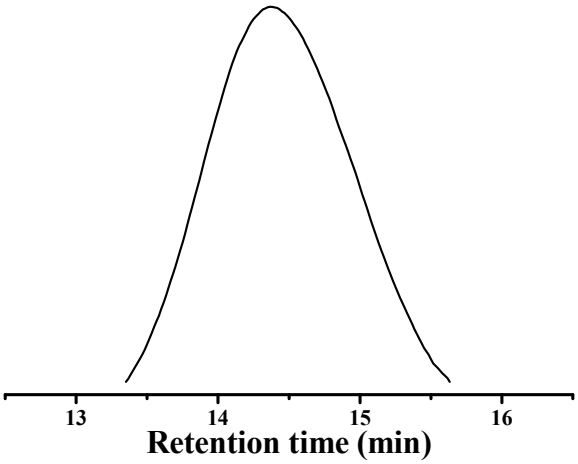

Figure S25. GPC curve of Ppdc.

2. Supporting Tables

Table S1. The $^5D_4$ lifetimes (τ) of Eu_xTb_y-Ppdc monitored at 543 nm and energy-transfer efficiency from Tb^{3+} to Eu^{3+} ions (E).

Eu:Tb	8:2	6:4	5:5	4:6	2:8
τ (ms)	1.20	1.45	1.49	1.51	1.53
E	25.0%	9.4%	6.8%	5.6%	4.3%

Table S2. The assignments of FT-IR spectra of Eu-Ppdc before (A) and after (B) exposure to TEA vapor in Figure S17.The unit of wavenumber is cm^{-1}.

Assignment	C=O (amide I)	C=N
A	1636	1564
B	1657	1540

Table S3. The fracture energy evaluated from the curves in the Figure S20.

Sample	Original Before	Healed Before	Original After	Healed After
Fracture Energy ($MJ\ m^{-3}$)	1.78	1.43	1.66	1.23

References

(1) Kotova, O.; Daly, R.; dos Santos C. M.; Boese, M.; Kruger, P. E.; Boland, J. J.; Gunnlaugsson, T., Europium - Directed Self - Assembly of a Luminescent Supramolecular Gel from a Tripodal Terpyridine - Based Ligand. *Angew. Chem. Int. Ed.* **2012**, *51*,7208-7212.

(2) Martínez-Calvo, M.; Kotova, O.; Möbius, M. E.; Bell, A. P.; Mccabe, T.; Boland, J. J.; Gunnlaugsson, T., Healable Luminescent Self-Assembly Supramolecular Metallogels Possessing Lanthanide (Eu/Tb) Dependent Rheological and Morphological Properties. *J. Am. Chem. Soc.* **2015,** *137*, 1983-1992.

(3) Wang, T.; Li, P.; Li, H., Color-Tunable Luminescence of Organoclay-Based Hybrid Materials Showing Potential Applications in White LED and Thermosensors. *ACS Appl. Mater. Interfaces* **2014,** *6*, 12915-12921.

(4) Xu, Q.; Li, Z.; Li, H., Water-Soluble Luminescent Hybrid Composites Consisting of Oligosilsesquioxanes and Lanthanide Complexes and their Sensing Ability for Cu^{2+}. *Chem. Eur. J.* **2016,** *22*, 3037-3043.